Dislocation dynamics in an anisotropic stripe pattern

Carina Kamaga, Fatima Ibrahim, and Michael Dennin
Department of Physics and Astronomy, University of California, Irvine, Irvine, California 92696-4575, USA
(Received 5 January 2004; published 15 June 2004)

The dynamics of dislocations confined to grain boundaries in a striped system are studied using electroconvection in the nematic liquid crystal N4. In electroconvection, a striped pattern of convection rolls forms for sufficiently high driving voltages. We consider the case of a rapid change in the voltage that takes the system from a uniform state to a state consisting of striped domains with two different wave vectors. The domains are separated by domain walls along one axis and a grain boundary of dislocations in the perpendicular direction. The pattern evolves through dislocation motion parallel to the domain walls. We report on features of the dislocation dynamics. The kinetics of the domain motion is quantified using three measures: dislocation density, average domain wall length, and total domain wall length per area. All three quantities exhibit behavior consistent with power-law evolution in time, with the defect density decaying as $t^{-1/3}$, the average domain wall length growing as $t^{1/3}$, and the total domain wall length decaying as $t^{-1/5}$. The two different exponents are indicative of the anisotropic growth of domains in the system.

DOI: 10.1103/PhysRevE.69.066213 PACS number(s): 89.75.Kd, 47.54.+r, 64.60.Cn

I. INTRODUCTION

The dynamics of topological defects are observed to dominate the temporal evolution of patterns in many physical systems. However, our understanding of the quantitative contribution of the defect dynamics to the evolution of patterns is still not complete. One area in which topological defects potentially play a central role is the growth of domains in a patterned system after a sudden change in the external parameters. For many striped systems, such as diblock copolymers and convection in fluids, many of the topological defects (such as disclinations and domain walls) are the same as those that exist in classic models for the growth of "uniform domains," such as Ising models or *x-y* models [1]. For uniform systems, the contribution of the topological defects to the time evolution of the domains is relatively well understood [2], whereas this is not the case for striped systems.

It is useful to briefly review the situation for uniform domain growth [2]. One is generally interested in the evolution of a system after a rapid change of an external parameter, or a quench. Typically, one considers an initially uniform state that immediately after the quench is no longer an equilibrium or steady-state phase of the system. The new equilibrium phase is degenerate, and domains of the different states form. For example, in an Ising system, one would have domains of up and down spins. During the subsequent evolution of the system, or *coarsening*, the domains are characterized by a single length scale. This length grows as a power of time t^n, where n is the growth exponent. We use the designation "uniform domains" to refer to systems in which, within a domain, the system is uniform. Examples of this type of system include magnetic systems, metallic alloys, binary fluids, and nematic liquid crystals [2]. One of the main goals of this field is to understand the possible values of n and other features of the late time scaling. For uniform systems, much of the late-time behavior can be understood in terms of the topological defects of the order parameter [2]. For most cases, the growth exponent is $1/3$ if the order parameter is conserved, such as in binary fluids, and the exponent is $1/2$ if it is not conserved, as in magnetic systems [2]. Various interesting alternate cases exist, especially for the *x-y* model in one and two dimensions [2]. In contrast, no similar general framework exists for patterned domains. These are systems in which, within a domain, the system exhibits a pattern, such as stripes.

Stripes, or more generally patterns, occur in a wide range of systems [1,3], including convecting fluids, animal coats, polymer melts, and ferromagnets. Stripes occur both as an equilibrium state of the system, such as in diblock copolymers, and as a result of external driving, as in convection in fluids. A sudden change of an external parameter, a *quench*, can bring the system from a spatially uniform state to a striped state that undergoes coarsening, or phase ordering. The coarsening of striped domains has focused on *isotropic* systems [4–9], with a significant fraction of the work focusing on simulations of model equations, such as the Swift-Hohenberg equation [4–6,8,10]. Experimental work has been limited to two systems, one isotropic (diblock copolymers [7,9]) and one anisotropic (electroconvection in nematic liquid crystals [11,12]). For isotropic systems, the stripes can have any orientation. In this case, the dominant defects are disclinations and domain walls, though dislocations are observed as well. For diblock copolymers, the measured growth exponent is consistent with $n=1/4$. Detailed studies of the disclination dynamics are able to explain this measured exponent [7,9].

For simulations of isotropic systems, growth exponents are usually consistent with $1/4$ [4–6] or $1/5$ [4–6,11]. Factors affecting the measured exponent include external noise and the quantity used to characterize the domains. There is evidence that for small enough quench depths the growth exponent is $1/3$ [8,10,13]. An open question is the connection between the simulations and experiments with the diblock copolymer systems. The dominant defects appear to be different between the simulations and experiment, leaving open the question of a general explanation for the coarsening behavior.

For electroconvection (an anisotropic system), two main classes of patterns occur as the initial transition: normal and oblique rolls [14–16]. Electroconvection uses a nematic liquid crystal. The molecules of a liquid crystal align on average along a particular axis, referred to as the director [17]. Normal rolls consist of a system of parallel rolls oriented with the wave vector parallel to the director field (the average axis of alignment for the molecules). The main defect in the normal roll regime is isolated dislocations. The dynamics of these dislocations have been studied both experimentally and theoretically [18–21], though not in the context of domain growth. Oblique rolls correspond to stripes in which the wave vector forms a nonzero angle with respect to the undistorted director field. In the oblique roll regime, a quench typically produces a pattern consisting of domains of stripes with only two orientations, referred to as zig and zag rolls. In this case, the main defects are domain walls and dislocations. For a particular case of electroconvection, growth exponents of $1/4$ were observed [11]. However, in contrast to isotropic systems, disclinations were not present in this system. Again, this points to the need to better understand the dynamics of the various classes of defects if a general framework for understanding phase ordering in pattern forming systems is to emerge.

In considering the existing work, there are at least two obvious questions. Given that the uniform and pattern forming systems exhibit similar topological defects, why are the resulting growth exponents so different? Given the range of growth exponents observed for pattern forming systems, can they even be explained in terms of the dynamics of topological defects? An important step in answering both of these questions is elucidation of the defect dynamics. The work with diblock copolymers has already made important contributions along these lines for disclinations. In this paper, we focus on the dynamics of confined dislocations found in the oblique roll regime of electroconvection [21].

Figure 1(b) is a top view of a pattern in an electroconvection cell that illustrates the defects of interest in this paper. The cell consists of a nematic liquid crystal confined between specially treated glass plates that align the director parallel to the plates along a single axis. This axis is defined to be the x axis, or horizontal direction. The y axis, or vertical direction, is also parallel to the glass plates, but perpendicular to the undistorted director. The z axis is taken perpendicular to the plates. The nematic liquid crystal is doped with ionic impurities. An ac voltage is applied perpendicular to the plates. There exists a critical value of the applied voltage V_c at which a transition from a spatially uniform state to a striped state occurs. The striped state consists of convection rolls with a corresponding periodic variation of the director and charge density. As shown in Fig. 1, we studied the case of *oblique rolls*, and the two classes of topological defects are domain walls and dislocations. The dislocations are special in that they are mostly confined to vertical domain walls. Disclinations do not occur, as the stripes are not easily curved. As we will show, the domain walls are essentially static, so only the dynamics of the dislocations are of interest. In this paper, we report on qualitative features of the dislocation dynamics and their interactions. In addition, we will report on the time dependance of three global measures of defect kinetics: dislocation density, average domain wall length, and total domain wall length per area. The rest of the paper is organized as follows. Section II describes the experimental details. Section III presents the results, and Sec. IV is a summary and discussion of the results.

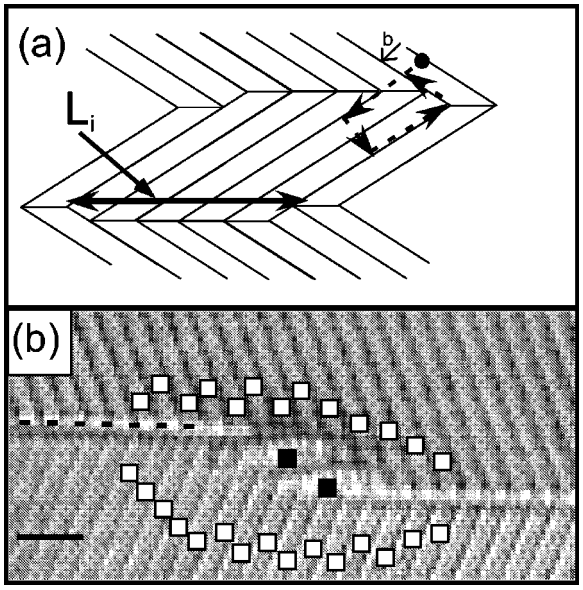

FIG. 1. (a) A schematic drawing illustrating a transition from a zig to a zag and back to a zig region of the system. The black lines represent lines of constant phase between the stripes. There are two horizontal domain walls, one at each transition. Also, one example of each type of step dislocation is shown. The Burgers vector is also illustrated for one of the dislocations. The length of a horizontal domain wall is indicated by L_i. (b) A close-up of a section of the system that shows two step dislocations (black squares). The white squares are provided as an aid in counting the zig and zag rolls. One finds that there are two more zig rolls than zag, as expected with two dislocations. The dashed line highlights one of the horizontal domain walls. The scale bar represents 0.15 mm.

II. EXPERIMENTAL DETAILS

The details of the experimental apparatus are described in Ref. [22]. The nematic liquid crystal N4 was doped with 0.1 wt% of tetra *n*-butylammonium bromide $[(C_4H_9)4NBr]$. Commercial cells [23] with a quoted thickness of 23 μm and 1 cm^2 electrodes were used, giving an aspect ratio of 435. The average wavelength of the rolls was 51 μm. The sample temperature was maintained at $30.0 \pm 0.002\,^{\circ}C$. The patterns were observed from above using a modified shadowgraph setup [22,24,25] that emphasized the contrast between zig and zag rolls. The magnification was chosen to monitor the largest possible area of the sample while maintaining enough resolution to resolve the stripe pattern. The area imaged contained approximately 150 rolls.

All of the results reported here are for a fixed quench depth of $\epsilon = V^2/V_c^2 - 1 = 0.05$. After a quench, domains of zig and zag rolls form within 60 s. [The relevant relaxation times for electroconvection are the director relaxation time (0.6 s) and the charge relaxation time $(4 \times 10^{-5}\text{s})$.] The do-

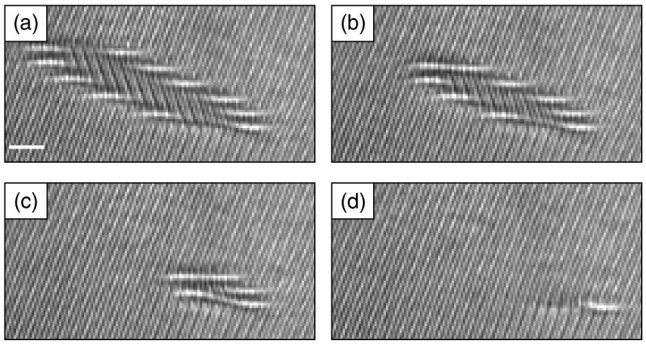

FIG. 2. Four images separated by 60 s illustrating the collapse of a zig domain. The scale bar represents 0.15 mm.

mains are separated by two classes of grain boundaries. There are domain walls that extend horizontally. Across these grain boundaries, the phase of the stripes is continuous. The vertical grain boundaries consist of discrete steps that are formed by dislocations. Each step contains either an extra zig or zag roll. Both grain boundaries are illustrated in Fig. 1, schematically in Fig. 1(a) and using an actual image of the system in Fig. 1(b). Figure 1(a) illustrates the Burgers vector construction for one of the dislocations, demonstrating the extra 2π of phase that occurs when traversing a closed path around the dislocation core. Vertical boundaries on opposite sides of a domain are always composed of dislocations of opposite sign. Also shown is the definition of the domain wall length L_i used later in the analysis of coarsening.

The dislocation number density $\rho(t)=n(t)/A$ was measured by counting the number of dislocations $[n(t)]$ in a fixed viewing area A. Because of the resolution used to take the images and the fact that the defects were in such close proximity to each other within the domain walls, the defects were counted by hand. At each time, $\rho(t)$ was averaged over ten different quenches. For the same times, we measured the length of the individual horizontal domain walls in the system, L_i [see Fig. 1(a)]. From this, we computed both the average horizontal wall lengths $[\langle L\rangle=(1/N)\Sigma L_i$, where N is the number of horizontal walls] and the total domain wall length per area $[L=(1/A)\Sigma L_i]$. Both of these quantities were averaged over seven quenches. The results are plotted in Fig. 8, below. Here time is scaled by the director relaxation time $\tau_d=0.6$ s [14]. In order to avoid issues of the initial growth of the amplitude and wave number, we only considered times greater than $400\tau_d$. After this time, the average wave number changed by less than 0.3%.

III. RESULTS

The first obvious difference between this system and previous experiments [7,11] is the dramatic anisotropy of the growth. The dislocations in the vertical grain boundaries move essentially horizontally. Some discrete steps in the vertical direction are observed. This is very different from the usual glide or climb of a dislocations. This is best seen in a movie of the motion. An archived movie made from snapshots taken every 60 s and with a playback rate of 0.3 s/frame can be found in Ref. [26]. This horizontal motion is directly responsible for changes in the horizontal length scale of the domains.

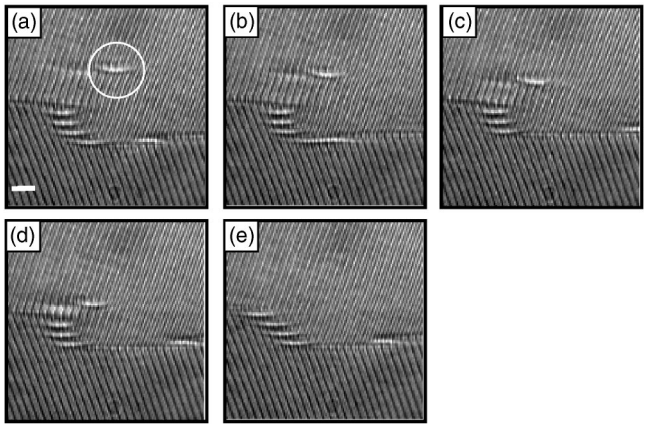

FIG. 3. Images separated by 150 s illustrating the incorporation of an isolated dislocation into a domain wall. The scale bar represents 0.15 mm.

In contrast to the dislocations, the horizontal grain boundaries are effectively stationary. Any vertical "motion" of domain boundaries occurs when an individual horizontal grain boundary is eliminated. This elimination occurs when the oppositely charged dislocations that form the domain wall's end points (see Fig. 1) annihilate. If only a single pair of end points annihilate, one has a discrete change of the vertical length by 49 μm. This step size is set by the step height corresponding to one dislocation in a vertically orientated domain wall. In order to eliminate a domain completely, the entire set of oppositely changed dislocations that form the vertical walls must annihilate each other. This is illustrated by the series of snapshots in Fig. 2 taken from the archived movie [26]. In this case, the number of dislocations on each side of the domain differs by 1. After the elimination of the

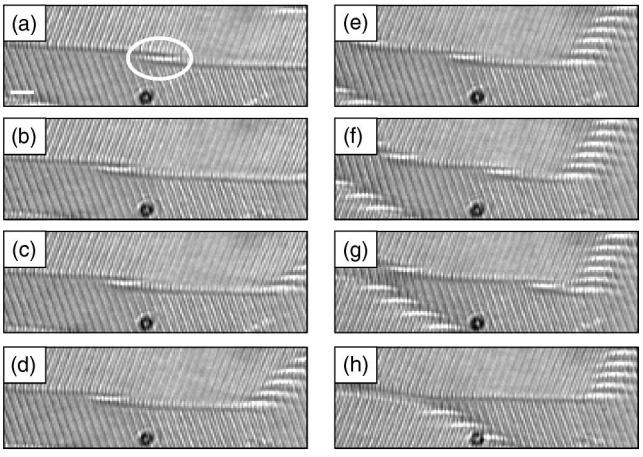

FIG. 4. Eight images separated by 300 s illustrating the motion of a single dislocation highlighted by a circle in (a). A dust particle on the surface of the sample is not removed to provide a frame of reference. In (a)–(d), the dislocation oscillates. In (e)–(h), the dislocation is attracted to one of opposite sign and annihilated. The scale bar represents 0.15 mm.

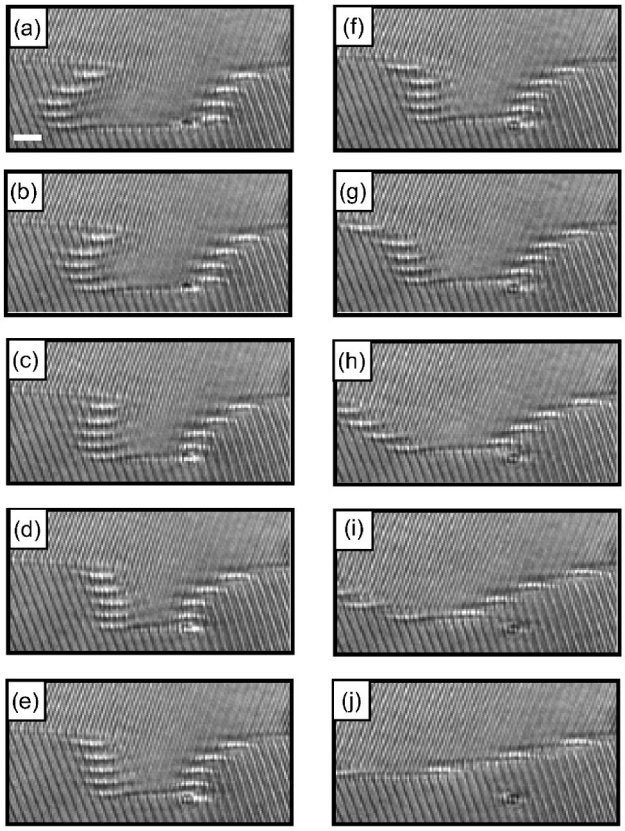

FIG. 5. Images separated by 150 s illustrating oppositely charge dislocations moving together, "bouncing," and ultimately attracting each other. One can also observe the spread of dislocations in a vertical wall that is highlighted in Fig. 6. The scale bar represents 0.15 mm.

domain, a single dislocation remains. Many domains contained equal numbers of dislocations, producing no isolated dislocations.

There are a small number of isolated dislocations, as seen in Fig. 2. These dislocations move through the sample either by climbing or gliding. Isolated dislocation either eventually move into a domain wall or annihilate with an oppositely charged dislocations in a domain wall. Figure 3 is a series of snapshots taken from the archived movie [26] that illustrate the incorporation of an isolated dislocation into a domain wall. This is consistent with the behavior of isolated dislocation predicted in Ref. [21]. They rarely annihilate with other isolated dislocations because of their extremely low density.

During the evolution process, the dislocations often exhibit behavior substantially more complex than that shown in Fig. 2. For example, Figs. 4(a)–4(d) illustrates a case in which a single dislocation in a domain wall is observed to be undergoing oscillatory motion. Eventually, this defect is close enough to an oppositely charged defect that it accelerates toward that defect and is annihilated [Figs. 4(e)–4(h)]. Figure 5 illustrates another interesting behavior. (This event is can also be found in the archived movie [26].) Entire walls of oppositely charged defects can approach within some distance and then move apart. In a simple picture, oppositely charged defects would attract each other and such a bounce would not be possible. However, these defects are not isolated, and one must account for the entire field of defects to describe these more complicated motions. This is outside the scope of this paper and will be the subject of future work. One also observes initially coherent walls of dislocations undergoing dispersion as they move (Fig. 6). This separation of dislocations occurs because the details of the interactions result in dislocations within a wall moving with different speeds. Finally, an extremely rare event is the nucleation of a new zig or zag domain. What is interesting is that extremely thin domains are possible in which the horizontal walls are slightly curved and the ends contain dislocations (see Fig. 7).

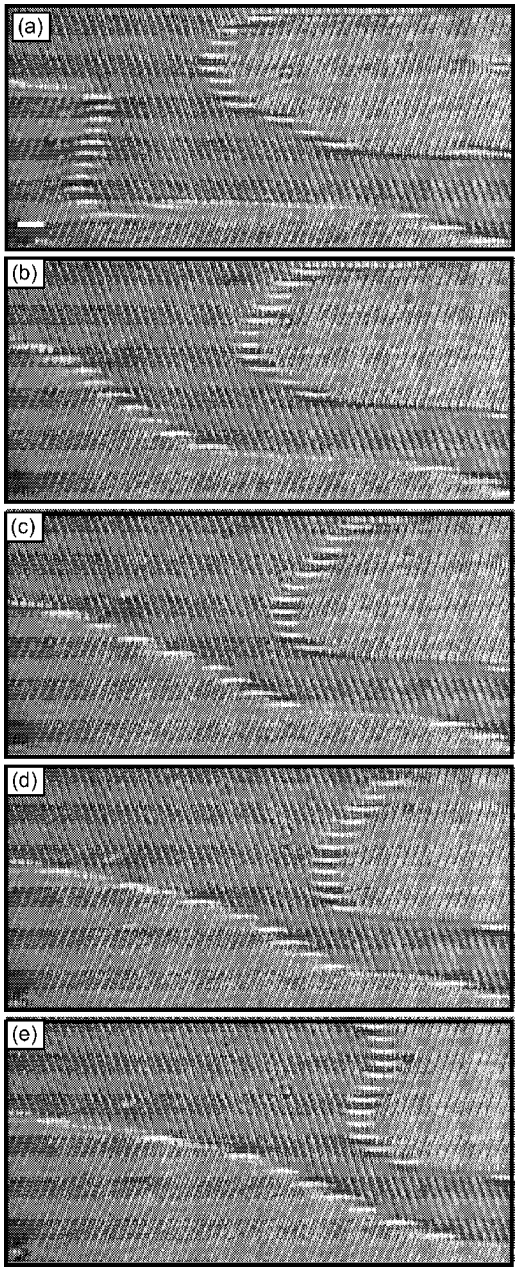

FIG. 6. Images separated by 300 s illustrating dislocations in a domain wall spreading out in time. The scale bar represents 0.15 mm.

Given the complex nature of the dislocation dynamics, for the purposes of this paper, quantitative measures focused on

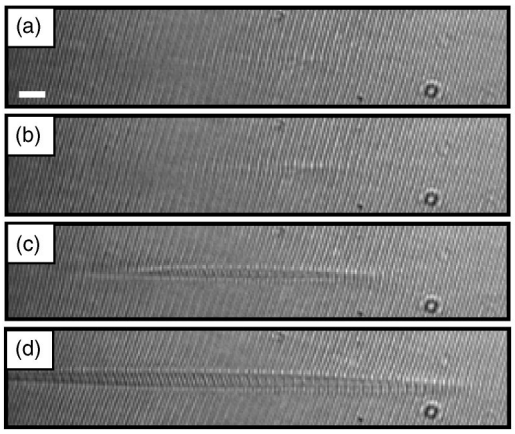

FIG. 7. Images separated by 150 s illustrating the nucleation of narrow domain without a dislocation pair. The scale bar represents 0.15 mm.

the time dependence of global quantities. The three quantities of interest are the dislocation density, the domain wall density, and the total domain wall length. The time dependence of these quantities is able to provide information about the rate of ordering along the axes parallel and perpendicular to the director. The results are summarized in Fig. 8.

One observes that all of the quantities are consistent with power-law growth after $t \approx 1000\tau_d$. Fits of the data in this regime give $\rho \sim t^{-0.32\pm0.02}$, $L \sim t^{-0.18\pm0.07}$, and $\langle L \rangle \sim t^{0.33\pm0.02}$. With the limited range that we are able to observe, it is difficult to show conclusively that a scaling regime has been reached. However, two conclusions are clear: (a) the growth is anisotropic and is best described by at least two different exponents, and (b) the exponents are different from previously studied striped systems [7,11]. The first point is illustrated in Fig. 8(c), where the dashed line has a slope of $-1/3$. The second point is illustrated by the dashed curves in Figs. 8(a) and 8(b). Here, the dashed curves represent the previously observed growth exponent of $1/4$.

Given that the defect motion is essentially confined to the horizontal (or x) direction, we tested for the existence of two different growth exponents. Typically, for domain growth, the scaling hypothesis assumes all lengths are scaled by a single scale factor $R(t) \sim t^n$ and the area scales as R^2. For our system, because of the obvious anisotropy, we assume that horizontal lengths and vertical lengths of domains are scaled independently by scale factors $L_x \sim t^{n_x}$ and $L_y \sim t^{n_y}$, respectively. Therefore, the number of domains, c, in our fixed viewing area A scales as $c \sim A/(L_x L_y)$. Because the dislocations are confined to vertical walls, the number of defects is given by the number of domains times a typical vertical dimension of the domain: $n(t) \sim cL_y$. This gives $\rho(t) = n(t)/A \sim L_y/(L_x L_y) \sim t^{-n_x}$. The average horizontal domain wall length ($\langle L \rangle$) scales as $\langle L \rangle \sim L_x \sim t^{n_x}$. As with the number of defects, the total horizontal domain wall length scales as cL_x. Therefore, the total domain wall length per viewing area will scale as $L \sim cL_x/A = L_x/(L_x L_y) \sim t^{-n_y}$. The results in Fig. 8 are consistent with two growth exponents $n_x = 1/3$ and $n_y = 1/5$, with the growth in the vertical direction being substantially slower than the growth in the horizontal direction. Here, the

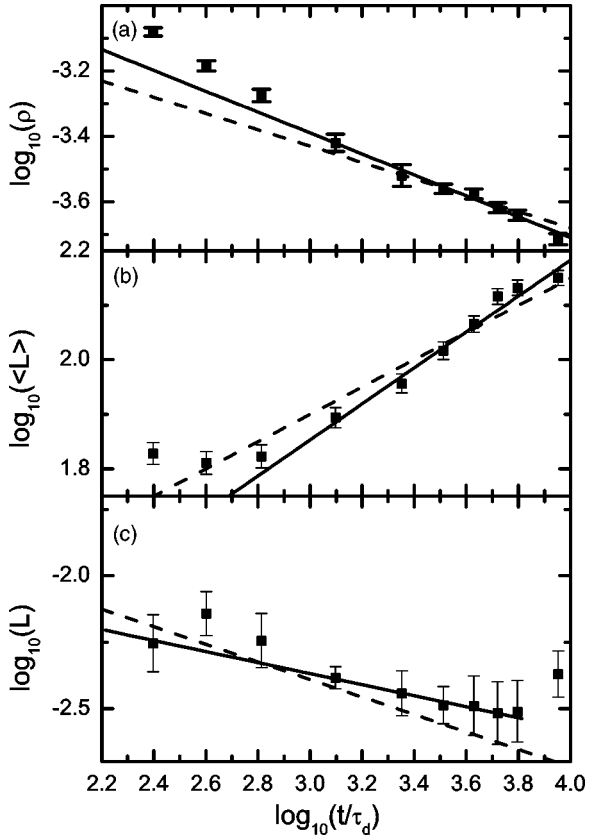

FIG. 8. (a) Plot of $\log_{10}(\rho)$ versus $\log_{10}(t)$. Symbols are experimental data. The solid line has a slope -0.32. For comparison, the dashed line has a slope of -0.25. (b) Plot of $\log_{10}(\langle L \rangle)$ versus $\log_{10}(t)$. Symbols are experimental data. The solid line has a slope 0.33. For comparison, the dashed line has a slope of 0.25. (c) Plot of $\log_{10}(L)$ versus $\log_{10}(t)$. Symbols are experimental data. The solid straight line has slope of -0.2. For comparison, the dashed line in (c) has a slope of -0.33.

time dependences of $\rho(t)$ and $\langle L \rangle$ provide independent measures of n_x.

Another issue is the impact of the finite viewing window, which determines the maximum time for which we can view the system. This is seen in Fig. 8(c), where the possible scaling of $L(t)$ breaks down for $t > 5000\tau_d$, even though the other measures still exhibit possible scaling. This is understandable because this is the time when most horizontal boundaries extend across our field of view and yet contain significant numbers of step dislocations of opposite sign. Therefore, as these dislocations annihilate with each other, both $\rho(t)$ and $\langle L \rangle$ continue to evolve, while $L(t)$ remains effectively constant.

IV. SUMMARY

We report observations of the dynamics of an interesting class of dislocations: dislocations confined to vertically oriented domain walls between two degenerate oblique rolls. The dislocations exhibit highly nontrivial behavior, forming coherent grain boundaries, exhibiting motion that is neither climb nor glide, and executing interesting dynamics, includ-

ing oscillations. The motion of isolated dislocations toward the horizontal grain boundaries and the confinement of the dislocations to grain boundaries are expected on general arguments from amplitude equations [21]. However, existing theoretical work has focused on the horizontal domain walls and individual dislocations [21]. A more detailed theoretical and experimental study is required to understand the full range of the observed behavior. For example, it is clear that the observed dynamics are often due to the interactions of many dislocations.

Measures of the global properties of the topological defects provide some insight into the phase ordering of this system. On the one hand, the combination of anisotropy and stripes results in a relatively simple system. There are only two classes of defects (domain walls and dislocations), and their basic motions are straightforward. The dislocations move horizontally, and the domain walls are essentially stationary. This suggests that the phase ordering should be relatively straightforward to understand. On the other hand, the system is an interesting example of how stripes can make the system more complicated than the standard uniform systems. This is best seen by comparing the system to two standard universality classes for phase ordering in uniform systems: Ising and *X*-*Y* models.

Aspects of the electroconvection patterns are analogous to an Ising system — i.e., a system of spins with two states. In our system, the two states are the zig and zag rolls, and the horizontal domain walls are the topological defects one would expect in an Ising system. However, the presence of the stripes results in additional topological defects: dislocations. These defects are analogous to vortices in an *x*-*y* model — i.e., spins with any orientation in the plane — in that both vortices and dislocations have the same topological charge. In our system, they occur predominantly in vertical domain walls or as steps between two horizontal domain walls. Even with this ambiguity, because there is no obvious conservation law (both zig rolls and zag rolls are eliminated), one expects a growth exponent of $1/2$ for both the Ising and *X*-*Y* modes [2]. The observed growth for electroconvection is clearly slower, being consistent with $1/3$ in one direction and $1/5$ in the other. This suggests that the confined dislocations represent a new type of coarsening dynamics.

One direction that may provide further insight into the exact cause of the slower dynamics is comparisons with simulations of an anisotropic Swift-Hohenberg model [27]. Initial simulations are consistent with a growth exponent of $1/3$ for shallow quenches with pinning effects becoming important as a function of quench depth [27]. This will be the subject of future work.

ACKNOWLEDGMENTS

The authors wish to thank Ben Vollmayr-Lee, Denis Boyer, Eberhard Bodenschatz, and Werner Pesch for useful conversations. This work was supported by NSF Grant No. DMR-9975479. M.D. also thanks the Research Corporation and Alfred P. Sloan Foundation for additional funding for this work.

[1] M. C. Cross and P. C. Hohenberg, Rev. Mod. Phys. **65**, 851 (1993).
[2] A. J. Bray, Adv. Phys. **43**, 357 (1994).
[3] J. P. Gollub and J. S. Langer, Rev. Mod. Phys. **71**, S396 (1999).
[4] K. R. Elder, J. Vinals, and M. Grant, Phys. Rev. Lett. **68**, 3024 (1992).
[5] M. C. Cross and D. I. Meiron, Phys. Rev. Lett. **75**, 2152 (1995).
[6] J. J. Christensen and A. J. Bray, Phys. Rev. E **58**, 5364 (1998).
[7] C. Harrison, D. H. Adamson, Z. Cheng, J. Sebastian, S. Sethuraman, D. Huse, R. A. Register, and P. M. Chaikin, Science **290**, 1558 (2000).
[8] D. Boyer and J. Vinals, Phys. Rev. E **64**, 050101 (2001).
[9] C. Harrison, Z. Cheng, S. Sethuraman, D. A. Huse, P. M. Chaikin, D. A. Vega, J. M. Sebastian, R. A. Register, and D. H. Adamson, Phys. Rev. E **66**, 011706 (2002).
[10] H. Qian and F. Mazenko, Phys. Rev. E **67**, 036102 (2003).
[11] L. Purvis and M. Dennin, Phys. Rev. Lett. **86**, 5898 (2001).
[12] C. Kamaga, D. Funfschilling, and M. Dennin, Phys. Rev. E (to be published).
[13] D. Boyer and J. Vinals, Phys. Rev. E **65**, 046119 (2002).
[14] E. Bodenschatz, W. Zimmermann, and L. Kramer, J. Phys. (Paris) **49**, 1875 (1988).
[15] I. Rehberg, B. L. Winkler, M. de la Torre Juárez, S. Rasenat, and W. Schöpf, Festkoerperprobleme **29**, 35 (1989).
[16] L. Kramer and W. Pesch, Annu. Rev. Fluid Mech. **27**, 515 (1995).
[17] P. G. de Gennes and J. Prost, *The Physics of Liquid Crystals* (Clarendon Press, Oxford, 1993).
[18] G. Goren, I. Procaccia, S. Rasenat, and V. Steinberg, Phys. Rev. Lett. **63**, 1237 (1989).
[19] S. Rasenat, V. Steinberg, and I. Rehberg, Phys. Rev. A **42**, 5998 (1990).
[20] L. Kramer, E. Bodenschatz, and W. Pesch, Phys. Rev. Lett. **64**, 2588 (1990).
[21] L. Kramer, E. Bodenschatz, W. Pesch, W. Thom, and W. Zimmermann, Liq. Cryst. **5**, 699 (1989).
[22] M. Dennin, Phys. Rev. E **62**, 6780 (2000).
[23] E.H.C. CO., Ltd., 1164 Hino, Hino-shi, Tokyo, Japan.
[24] S. Rasenat, G. H. B. L. Winkler, and I. Rehberg, Exp. Fluids **7**, 412 (1989).
[25] H. Amm, R. Stannarius, and A. G. Rossberg, Physica D **126**, 171 (1999).
[26] See EPAPS Document No. E-PLEEE8-69-093406 for a movie of coarsening in progress. A direct link to this document may be found in the online article's HTML reference section. The document may also be reached via the EPAPS homepage (http://www.aip.org/pubservs/epaps.html) or from ftp.aip.org in the directory/epaps/ See the EPAPS homepage for more information.
[27] D. Boyer (private communication) (2003).